

Half-ordered state in the anisotropic Haldane-gap antiferromagnet $\text{Ni}(\text{C}_5\text{D}_{14}\text{N}_2)_2\text{N}_3(\text{PF}_6)$

A. Zheludev,^{1,*} B. Grenier,² E. Ressouche,² L.-P. Regnault,² Z. Honda,³ and K. Katsumata⁴¹Condensed Matter Sciences Division, Oak Ridge National Laboratory, Oak Ridge, Tennessee 37831-6393, USA²DRFMC/SPSMS/MDN, CEA-Grenoble, 17 rue des Martyrs, 38054 Grenoble Cedex, France³Faculty of Engineering, Saitama University, Urawa, Saitama 338-8570, Japan⁴The RIKEN Harima Institute, Mikazuki, Sayo, Hyogo 679-5148, Japan

(Received 11 November 2004; published 25 March 2005)

Neutron diffraction experiments performed on the Haldane gap material $\text{Ni}(\text{C}_5\text{D}_{14}\text{N}_2)_2\text{N}_3(\text{PF}_6)$ in high magnetic fields applied at an angle to the principal anisotropy axes reveal two consecutive field-induced phase transitions. The low-field phase is the gapped Haldane state, while at high fields the system exhibits a three-dimensional long-range Néel order. In a peculiar phase found in intermediate fields only half of all the spin chains participate in the long-range ordering, while the other half remain disordered and gapped.

DOI: 10.1103/PhysRevB.71.104418

PACS number(s): 75.10.-b, 75.25.+z, 75.10.Pq

High-field phase transitions in quantum antiferromagnets (AFs) have recently drawn a great deal of attention. Of particular interest is the field-induced spin freezing exhibited by many quantum spin liquids. The massive triplet of low-lying $S=1$ gap excitations (magnons) in such systems is subject to Zeeman splitting by external magnetic fields. A soft-mode quantum phase transition occurs when the gap for one member of the triplet is driven to zero. The result is a Bose condensation of magnons. In the presence of magnetic anisotropy and weak interchain interactions, always found in real materials, the magnetized high-field phase is a Néel-like state with an AF long-range order. The phase transition itself and the peculiarities of the high-field phase have been studied experimentally in several model materials, including the Haldane-gap antiferromagnets NDMAP $[\text{Ni}(\text{C}_5\text{D}_{14}\text{N}_2)_2\text{N}_3(\text{PF}_6)]^{1-7}$ and NDMAZ $[\text{Ni}(\text{C}_5\text{H}_{14}\text{N}_2)_2\text{N}_3(\text{ClO}_4)]^{8,9}$ the bond-alternating $S=1$ chain NTENP $[\text{Ni}[N,N'\text{-bis}(3\text{-aminopropyl})\text{propane-1,3-diamine}(\mu\text{-NO}_2)]\text{ClO}_4]$,¹⁰ and dimer systems such as TiCuCl_3 (Ref. 11) and $\text{Cs}_3\text{Cr}_2\text{Br}_9$.¹²

It has been long established that magnetic anisotropy, which is particularly important for $S=1$ materials, has a strong impact on the phase transition. The value of the critical field H_c depends on the relative orientation of the applied field and the anisotropy tensor.¹³⁻¹⁵ A very interesting case is that of NDMAP. This compound features two equivalent sets of Haldane spin chains with noncollinear local anisotropy axes. To date, all experiments were performed in magnetic fields applied along the principal axes of the orthorhombic crystal structure that are also the *macroscopic* magnetic anisotropy axes. In these geometries all tilts of the local anisotropy axes relative to the field direction are the same for the two chain types.⁵ In the present study we investigate a less symmetric scenario, in which the magnetic field is applied in a general direction relative to the crystal axes. We find *two* consecutive field-induced transitions from the quantum-disordered spin liquid to the ordered Néel phase, with a novel “half-ordered” phase in between.

The crystal structure of NDMAP (orthorhombic space group $Pn\bar{m}n$, $a=18.046$ Å, $b=8.705$ Å, and $c=6.139$ Å) was described in detail in Ref. 4. The $S=1$ chains run along the

crystallographic c axis. The in-chain exchange constant is $J=2.6$ meV. Interchain interactions are much weaker, $|J_\perp/J|<10^{-3}$. The magnetic anisotropy is predominantly of the single-ion easy-plane type with $D/J\approx 0.25$. In addition, there is a weak in-plane anisotropy term, and the degeneracy of the Haldane triplet is fully lifted. The gap energies for excitations polarized along the principal anisotropy axes x , y , and z are $\Delta_x=0.42(3)$ meV, $\Delta_y=0.52(6)$ meV, and $\Delta_z=1.9(1)$ meV.¹⁶ The anisotropy axes are determined by the geometry of the corresponding Ni^{2+} coordination octahedra and, as mentioned above, do *not* exactly coincide with the crystallographic directions. Instead, the x and z axes of the NiN_6 octahedra are in the (a,c) crystallographic plane, but tilted by $\alpha\approx 16^\circ$ relative to the a and c axes, respectively. There are two types of chains related by symmetry, and the corresponding tilt directions are opposite. Within each set of chains the Ni^{2+} sites form a simple orthorhombic Bravais lattice. On the other hand, the two sets of chains are displaced by $(0.5,0.5,0.5)$ relative to each other. The overall lattice of Ni^{2+} ions is thus a body-centered one. Due to this geometric frustration, the two sets of antiferromagnetic spin chains are magnetically decoupled at the mean-field level. The main features of the crystal structure of NDMAP are illustrated in Fig. 1.

Our neutron diffraction experiments were performed on a fully deuterated single crystal NDMAP sample of the approximate mass of 100 mg. The data were taken on the D23 lifting-counter diffractometer at Institut Laue-Langevin. The sample environment was a vertical-field cryomagnet with a dilution refrigerator insert. The data were taken at $T\sim 35$ mK in magnetic fields up to 6 T. Unfortunately, there was no possibility of rotating the sample *in situ* during the experiment. Remounting the sample to explore several orientations was not an option either, as the crystals are known to shatter and deteriorate rapidly during cooling and heating cycles. For this reason only one experimental geometry was realized, with the magnetic field applied at an angle $\psi=14.2^\circ$ to the c axis, in the (a,c) crystallographic plane, as shown in Fig. 1. For one set of spin chains that we will refer to as type A, the field was thus almost exactly parallel to the main anisotropy axis, the corresponding angle being

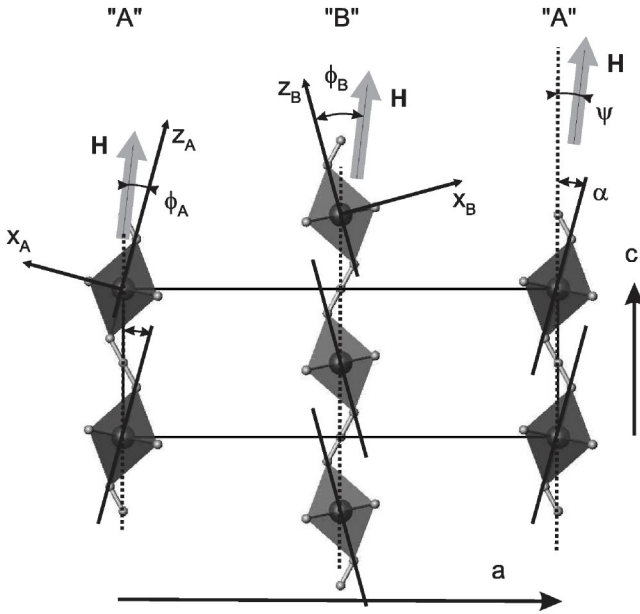


FIG. 1. Crystal structure of NDMAP in projection onto the (ac) crystallographic plane and the geometry of the present experiment. Only the N-ions (small balls) and Ni-ions (large balls) are shown. The local magnetic anisotropy axes x and z are tilted in the (ac) plane by $\alpha = 16^\circ$ relative to the c axis. The tilt direction is opposite for type-A and type-B chains. The field H is applied at an angle ψ relative to the c axis of the crystal and forms unequal angles ϕ_A and ϕ_B with the anisotropy axes z_A and z_B , respectively.

$\phi_B = \alpha - \psi = 1.8^\circ$. For type-B chains the angle between the field direction and the local Ni^{2+} anisotropy axes was considerably larger, $\phi_B = \alpha + \psi = 30.2^\circ$.

Our main experimental result is drawn from the measured field dependence of the $(0,0.5,0.5)$ and $(1,0.5,0.5)$ magnetic Bragg intensities at $T = 35$ mK. These data are plotted in Fig. 2. In the geometry of the present experiment *two* distinct anomalies are detected at $H_c^{(1)} = 3.4$ T and $H_c^{(2)} = 4.1$ T. Below $H_c^{(1)}$ there is no antiferromagnetic Bragg scattering in NDMAP that retains its spin-singlet ground state. At $H_c^{(1)}$ antiferromagnetic Bragg reflections simultaneously appear at both $(0,0.5,0.5)$ and $(1,0.5,0.5)$ reciprocal-space positions. These two peaks remain of roughly equal intensity in the field range $H_c^{(1)} < H < H_c^{(2)}$. Above the second transition at $H_c^{(2)}$ the intensity of the $(0,0.5,0.5)$ peak starts to increase more rapidly. In contrast, the $(1,0.5,0.5)$ peak intensity flattens out and even decreases slightly. Typical scans across the two magnetic Bragg reflections collected at $H = 6$ T are shown in the insets in Fig. 2.

Though a detailed determination of the magnetic structure has not been performed, a survey of several magnetic Bragg peaks at $H = 6$ T revealed a consistent intensity pattern. It was found that $(h+k+l)$ -even reflections are considerably stronger than the $(h+k+l)$ -odd ones. Within each of these reflection classes the intensity is a smooth function of wave vector transfer, typical of the combined effects of the magnetic form factor and neutron polarization factors. Such behavior is consistent with an almost collinear antiferromagnetic spin arrangement on a body-centered lattice, which was previously shown to be realized in NDMAP in high magnetic

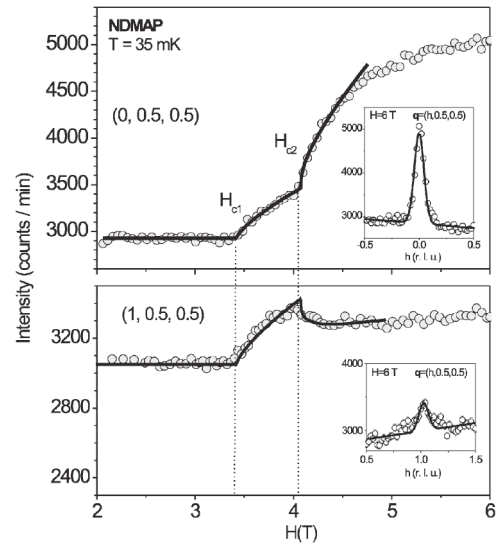


FIG. 2. Main panels: field dependence of two magnetic Bragg peak intensities measured in NDMAP at $T = 35$ mK. The magnetic field is applied in the (a, c) crystallographic plane at an angle 14.2° to the c axis. The solid lines are as described in the text. Insets: h -scans across the two magnetic Bragg peaks at $H = 6$ T.

fields applied strictly along the high-symmetry crystallographic directions.^{4,7}

The field-dependent behavior observed in the present study is in stark contrast to that previously seen for $H \parallel c$ (i.e., $\phi_A = \phi_B$), where only a single transition was detected. The unusual two-stage transition can be understood in the framework of a simple model proposed by Harada.¹⁷ The key idea is that long-range ordering occurs in each set of spin chains independently.

The critical fields for an individual spin chain in an arbitrarily directed magnetic field can be estimated using perturbation theory.^{18,19} Though clearly oversimplified, for a magnetic field applied parallel to any of the principal anisotropy axes this method is known to give the same values of H_c as more sophisticated calculations based on the quantum nonlinear sigma model¹⁵ or mapping to Majorana fermions.¹³ For a field in the (x, z) plane applied at an angle ϕ to the magnetic easy axis z , the perturbative result for H_c is⁷

$$\mu_B H_c = \sqrt{\frac{\Delta_x \Delta_y \Delta_z}{g_x^2 \Delta_x \sin^2 \phi + g_z^2 \Delta_z \cos^2 \phi}}. \quad (1)$$

In this formula g_z and g_x are components of the Ni^{2+} gyromagnetic tensor. Making use of the previously measured gyromagnetic ratios,¹ for the geometry of the present experiment one gets $H_c = 3.8$ T and $H_c = 4.3$ T for type-A and type-B chains, respectively. While somewhat larger than the measured values, these two fields can be associated with the two observed ordering transitions at $H_c^{(1)}$ and $H_c^{(2)}$.

Below $H_c^{(1)}$ both types of spin chains are in a quantum-disordered gapped state. As the external field exceeds $H_c^{(1)}$ at zero temperature, individual type-A chains acquire a long-range Néel order. Weak interactions between type-A chains stabilize this ordered state at nonzero temperatures and ensure the existence of true three-dimensional long-range static

antiferromagnetic spin correlations. Nevertheless, considering that interchain interactions are very weak, in the field range $H_c^{(1)} < H < H_c^{(2)}$ type-*B* chains must remain in the quantum-disordered gapped phase. The corresponding Ni^{2+} ions carry no static magnetization and do *not* participate in the long-range Néel order. This peculiar phase of NDMAP, where half the Haldane spin chains remain gapped while the other half participate in long-range antiferromagnetic order can be described as a “half-ordered” state. In this regime the only magnetized ions in NDMAP are located on type-*A* chains and form a simple Bravais lattice. As a consequence, (0,0.5,0.5) and (1,0.5,0.5) magnetic Bragg reflections have the same structure factor. Their intensities should differ only slightly due to slightly different form and polarization factors. These intensities are proportional to the square of the staggered magnetization on the *A* sublattice: $I_{(0,0.5,0.5)} \propto I_{(1,0.5,0.5)} \propto |m_A|^2$.

The situation changes at $H_c^{(2)}$ when the gap in type-*B* chains closes as well, and they too acquire static long-range AF spin correlations. Now static magnetic moments are located on both *A* and *B* sublattices, and they form a body-centered structure. In spite of geometric frustration, a definitive relative alignment between spins on the two sublattices is established via dipolar interactions and/or order-from-disorder fluctuation effects. The two magnetic Bragg peaks are then no longer equivalent. Assuming a collinear alignment of *A*- and *B*-type spins, their intensities are given by $I_{(0,0.5,0.5)} \propto |m_A + m_B|^2$ and $I_{(1,0.5,0.5)} \propto |m_A - m_B|^2$. As both staggered magnetizations increase with field, $I_{(0,0.5,0.5)}$ increases rapidly and $I_{(1,0.5,0.5)}$ levels off.

To construct a phenomenological semiquantitative description we can assume that $m_A = m_A^{(0)} |H/H_c^{(1)} - 1|^\beta \theta(H - H_c^{(1)})$ and $m_B = m_B^{(0)} |H/H_c^{(2)} - 1|^\beta \theta(H - H_c^{(2)})$. Assuming that the ordered moments on the two chain subsets are collinear (and thus the corresponding polarization factors for neutron scattering intensities are equal), the expression for the measured Bragg intensities can be written as

$$I_{(0,0.5,0.5)} \propto [m_A^{(0)} |H/H_c^{(1)} - 1|^\beta \theta(H - H_c^{(1)}) + m_B^{(0)} |H/H_c^{(2)} - 1|^\beta \theta(H - H_c^{(2)})]^2, \quad (2a)$$

$$I_{(1,0.5,0.5)} \propto [m_A^{(0)} |H/H_c^{(1)} - 1|^\beta \theta(H - H_c^{(1)}) - m_B^{(0)} |H/H_c^{(2)} - 1|^\beta \theta(H - H_c^{(2)})]^2. \quad (2b)$$

Fitting this form to the experimental data (solid lines in Fig. 2) yields the following parameters: $H_c^{(1)} = 3.42(1)$ T, $H_c^{(2)} = 4.07(1)$ T and $\beta = 0.37(2)$ and $m_A^{(0)}/m_B^{(0)} = 1.50(4)$. Overall, the experimentally measured field dependencies are rather well reproduced by the simple model.

The experimental observations of a two-stage transition and half-ordered state in NDMAP highlight several important aspects of field-induced spin freezing in highly anisotropic gap systems. First, the two-stage transition is a dramatic demonstration of the well known fact that gap energies and transition fields are influenced by *local* anisotropy parameters, rather than the macroscopic magnetic anisotropy routinely measured with bulk methods. The second conclusion is that the principal driving force of the phase transition is the tendency of individual spin chains to form a long-range Néel order at $T=0$ in sufficiently strong fields. Interchain interactions are of course needed to stabilize this order in three dimensions at $T>0$, but play only a minor role in determining the actual transition field at $T \rightarrow 0$. In future experiments it would be very interesting to investigate the angle dependence of the transition fields in NDMAP in more detail.

We would like to thank Professor Isao Harada at Okayama University for inspiring this experimental study and Dr. S. M. Shapiro at Brookhaven National Laboratory for his important contributions at an early stage of the project. Work at ORNL was supported by the U. S. Department of Energy under Contract No. DE-AC05-00OR22725. Work at RIKEN was supported in part by a Grant-in-Aid for Scientific Research from the Japan Society for the Promotion of Science.

*Electronic address: zheludevai@ornl.gov

¹Z. Honda, H. Asakawa, and K. Katsumata, Phys. Rev. Lett. **81**, 2566 (1998).

²Z. Honda, K. Katsumata, M. Hagiwara, and M. Tokunaga, Phys. Rev. B **60**, 9272 (1999).

³A. Zheludev, Y. Honda, Y. Chen, C. Broholm, K. Katsumata, and S. M. Shapiro, Phys. Rev. Lett. **88**, 077206 (2002).

⁴A. Zheludev, Z. Honda, C. Broholm, K. Katsumata, S. M. Shapiro, A. Kolezhuk, S. Park, and Y. Qiu, Phys. Rev. B **68**, 134438 (2003).

⁵A. Zheludev, S. M. Shapiro, Z. Honda, K. Katsumata, B. Grenier, E. Ressouche, L.-P. Regnault, Y. Chen, P. Vorderwisch, H.-J. Mikeska, and A. K. Kolezhuk, Phys. Rev. B **69**, 054414 (2004).

⁶M. Hagiwara, Z. Honda, K. Katsumata, A. K. Kolezhuk, and H.-J. Mikeska, Phys. Rev. Lett. **91**, 177601 (2003).

⁷Y. Chen, Z. Honda, A. Zheludev, C. Broholm, K. Katsumata, and

S. M. Shapiro, Phys. Rev. Lett. **86**, 1618 (2001).

⁸Z. Honda, K. Katsumata, H. A. Katori, K. Yamada, T. Ohishi, T. Manabe, and M. Yamashita, J. Phys.: Condens. Matter **9**, L83 (1997).

⁹A. Zheludev, Z. Honda, K. Katsumata, R. Feyerherm, and K. Prokes, Europhys. Lett. **55**, 868 (2001).

¹⁰Y. Narumi, M. Hagiwara, M. Kohno, and K. Kindo, Phys. Rev. Lett. **86**, 324 (2001).

¹¹C. Ruegg, N. Cavadini, A. Furrer, H.-U. Gudel, K. Kramer, H. Mutka, A. Wildes, K. Habicht, and P. Vorderwisch, Nature (London) **423**, 62 (2003).

¹²B. Grenier, Y. Inagaki, L. P. Regnault, A. Wildes, T. Asano, Y. Ajiro, E. Lhotel, C. Paulsen, T. Ziman, and J. P. Boucher, Phys. Rev. Lett. **92**, 177202 (2004).

¹³A. M. Tsvelik, Phys. Rev. B **42**, 10 499 (1990).

¹⁴I. Affleck, Phys. Rev. Lett. **65**, 2477 (1990).

- ¹⁵P. P. Mitra and B. I. Halperin, Phys. Rev. Lett. **72**, 912 (1994).
¹⁶A. Zheludev, Y. Chen, C. Broholm, Z. Honda, and K. Katsumata, Phys. Rev. B **63**, 104410 (2001).
¹⁷I. Harada (private communication).
¹⁸O. Golinelli, T. Jolicoeur, and R. Lacaze, J. Phys.: Condens. Matter **5**, 1399 (1993).
¹⁹L. P. Regnault, I. Zaliznyak, J. P. Renard, and C. Vettier, Phys. Rev. B **50**, 9174 (1994).